

## Studies on the Corrosion Inhibition of Copper in Nitric Acid Solution Using Some Pharmaceutical Compounds

A.M.Eldesoky<sup>1</sup>, Hala.M.Hassan<sup>2</sup>, A.S.Fouda<sup>3,\*</sup>

<sup>1</sup> Engineering Chemistry Department, High Institute of Engineering & Technology ( New Damietta), Egypt.

<sup>2</sup> Textile Technology Department, Industrial Education College, Beni-Suef University, Egypt and Chemistry Department, Faculty of Science, Jazan University, KSA

<sup>3</sup> Department of Chemistry, Faculty of Science, El-Mansoura University, El-Mansoura-35516, Egypt

\*E-mail: [asfouda@hotmail.com](mailto:asfouda@hotmail.com),

Received: 11 May 2013 / Accepted: 17 July 2013 / Published: 1 August 2013

---

The inhibition effect of some pharmaceutical compounds, on copper corrosion in 2 M HNO<sub>3</sub> at 30°C was investigated using potentiodynamic polarization, electrochemical impedance spectroscopy (EIS) and electrical frequency modulation (EFM) techniques as well as weight loss measurements. Tafel polarization studies have shown that these compounds suppress both the cathodic and anodic processes and thus these compounds act as mixed-type inhibitors. The results of EIS indicate that the presence of these compounds in the corrosive solutions decreases the double layer capacitance, increases the charge transfer resistance and inhibition efficiency. EFM can be used as a rapid and non destructive technique for corrosion rate measurements without prior knowledge of Tafel constants. The adsorption of these compounds on copper surface was found follows the Temkin's adsorption isotherm. The effect of temperature on corrosion inhibition has been studied and the thermodynamic activation and adsorption parameters were calculated to elaborate the mechanism of corrosion inhibition. The relationships between the inhibition efficiency and some quantum chemical parameters have been discussed.

---

**Keywords:** Copper- Corrosion- Quantum- Temkin- pharmaceutical compounds

### 1. INTRODUCTION

Copper has been one of more important materials in industry owing to its high electrical and thermal conductivities, mechanical workability and its relatively noble properties. It is widely used in many applications in electronic industries and communications as a conductor in electrical power lines, pipelines for domestic and industrial water utilities including sea water, heat conductors, heat

exchangers, etc. Therefore, corrosion of copper and its inhibition in a wide variety of media, have attracted the attention of many investigators [1- 10].

The use of inhibitors to minimize the loss of useful properties of metals or alloys due to corrosion when they attack chemically or electrochemically by its environment is one of the best known methods of corrosion protection. The structure of the inhibitor molecule is one of the major factors that influence the metal-inhibitor interaction [11]. For a metal like copper, which can form multi-bonds, inhibitor molecules containing N and S atoms are strongly recommended. Among the nitrogen-sulfur- or oxygen containing organic compounds is the heterocyclic compounds which are effective inhibitors for copper corrosion in aqueous solutions [12]. Many heterocyclic compounds containing the mercapto group have also been developed as copper corrosion inhibitors for different industrial applications [13]. Azole compounds contain nitrogen atoms, by which they coordinate with Cu (0), Cu (I) or Cu (II) through the lone pair electrons to form copper-azole complexes [14]. These complexes are generally believed to be polymeric in nature and form an adherent protective film on the copper surface, which acts as a barrier to aggressive ions such as chloride [14]. The efficiency of an azole inhibitor towards copper corrosion correlates with the semiconducting (p-and n-type) properties of the underlying copper (I) oxide [15]. In recent papers, different innocuously thiadiazole derivatives [16-23], have been reported as good inhibitors for copper or copper-based alloys corrosion in different corrosive media. Other studies indicated that azole compounds have been recognized as remarkably effective inhibitors for copper and brasses [24-28]. Due to the toxicity of widely used corrosion inhibitors and the ever tightening environmental regulations surrounding their use and disposal, there is great interest in replacing harmful inhibitors with effective non-hazardous alternatives. Over the past two decades, extensive research and development have led to the discovery of new classes of corrosion inhibitors, and the importance on the use of several drugs as corrosion inhibitors has grown. The aim of the paper is to investigate the effect of addition of some pharmaceutical compounds on the corrosion resistance of copper in 2 M HNO<sub>3</sub>. The electrochemical behavior of copper in nitric acid solutions with and without the presence of these pharmaceutical compounds is characterized by Tafel, EIS and EFM techniques as well as weight loss method. These compounds are nontoxic and inexpensive.

## **2. EXPERIMENTAL DETAILS**

### *2.1. Materials*

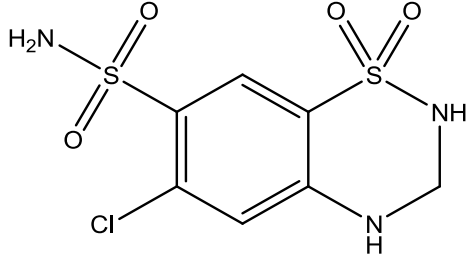
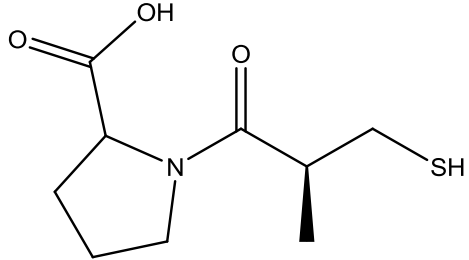
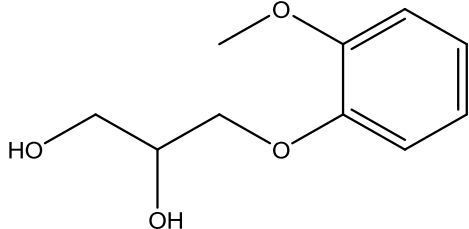
The experiments were performed with BDH copper specimens (pure, 99.9%)

### *2.2. Solutions*

The aggressive solutions used were made of AR grade HNO<sub>3</sub> (6 M) and its concentration was checked using standardized NaOH. Appropriate concentration (2 M) of acid was prepared by dilution using bidistilled water. 100 ml stock solutions (10<sup>-3</sup> M) of investigated pharmaceutical compounds were prepared by dissolving an accurately weighed quantity of each material in an appropriate volume

of absolute ethanol, then the required concentrations ( $1 \times 10^{-6}$  -  $11 \times 10^{-6}$  M) were prepared by dilution with bidistilled water.

**Table 1.** The molecular structures, names, molecular weights and molecular formulas of the investigated pharmaceutical compounds

Comp.	Structure	Name	Mol. Weight & Mol. Formula
(I)		6-Chloro-1,1-dioxo-3,4-dihydro-2H-1,2,4-benzothiadiazine-7-sulfonamide	297.74
(II)		1-((S)-3-mercapto-2-methylpropanoyl)pyrrolidine-2-carboxylic acid	217.29
(III)		3-(2-methoxyphenoxy)propane-1,2-diol	198.22

### 2.3. Experimental procedures

The weight loss experiments were carried out using copper coupons each of size 2 x 2 x 0.2 cm. The coupons were abraded, dried and weighted ( $W^\circ$ ), and then suspended in 100 ml solution of  $HNO_3$  without and with different concentrations of investigated pharmaceutical compounds for exposure period (3 hours). At the end of tests, the coupons were rinsed with bidistilled water, dried between two tissue papers, and weighed again ( $W$ ).

The inhibition efficiency (%IE) and the degree of surface coverage ( $\theta$ ) of investigated compounds on the corrosion of copper were calculated from equation (1):

$$\%IE = \theta \times 100 = [(W^\circ - W) / W^\circ] \times 100 \quad (1)$$

All Electrochemical measurements (potentiodynamic polarization, EIS and EFM techniques) were performed in a typical three compartment glass cell consisted of the copper specimen as working electrode (copper specimen was mounted in glass rod with an exposed area of  $1\text{cm}^2$ . An epoxy resin was used to fill the space between glass rod and copper electrode), platinum sheet as counter electrode ( $1\text{cm}^2$ ), and a saturated calomel electrode (SCE) as reference electrode. Prior to each experiment, the

specimen was abraded with a series of emery papers of different grit sizes up to 1200, washed several times with bidistilled water then with acetone and dried. The electrode potential was allowed to stabilize to 30 min. before starting the measurements. All experiments were conducted at room temperature.

Potentiodynamic polarization curves were obtained by changing the electrode potential automatically from (-500 to +400 mV) versus open circuit potential with a scan rate of  $1 \text{ mVs}^{-1}$ . % IE and the degree of surface coverage ( $\theta$ ) were calculated from equation (2):

$$\% \text{ IE} = \theta \times 100 = [(i_{\text{corr}} - i_{\text{corr(inh)}}) / i_{\text{corr}}] \times 100 \quad (2)$$

where  $i_{\text{corr}}$  and  $i_{\text{corr(inh)}}$  are the uninhibited and inhibited corrosion current density values, respectively, determined by extrapolation of Tafel lines to the corrosion potential.

Electrochemical impedance spectroscopy (EIS) measurements were carried out in a frequency range of 100 KHz to 10 mHz with amplitude of 5 mV peak-to-peak using ac signals at respective corrosion potential.

The inhibition efficiency (% IE) and the surface coverage ( $\theta$ ) of the used inhibitors obtained from the impedance measurements can be calculated from equation (3):

$$\% \text{ IE} = \theta \times 100 = [1 - (R_{\text{ct}}^{\circ} / R_{\text{ct}})] \times 100 \quad (3)$$

where  $R_{\text{ct}}^{\circ}$  and  $R_{\text{ct}}$  are the charge transfer resistance in the absence and presence of inhibitor, respectively.

Electrochemical frequency modulation (EFM) carried out using two frequencies 2 and 5 Hz. The base frequency was 1Hz with 32 cycles, so the waveform repeats after 1s. A perturbation signal with amplitude of 10mV was used for both perturbation frequencies of 2 and 5 Hz. The choice for the frequencies of 2 and 5 Hz was based on three principles<sup>[29]</sup>.

Measurements were performed with a Gamry instrument Potentiostat /Galvanostat /ZRA, (PCI300/4) this includes a Gamry framework system based on the ESA 400, Gamry applications that include DC105 software for DC corrosion measurements, EIS300 software for EIS measurements and EFM140 software for EFM measurements. Echem Analyst software was used for plotting, graphing and fitting data. A computer was used for collecting data.

#### 2.4. Theoretical study

All the quantum calculations were performed with complete geometry optimization using Accelrys Material Studio 4.4 software package.

### 3. RESULTS AND DISCUSSION

#### 3.1.1 Weight loss measurements

The weight loss of copper specimen in 2 M  $\text{HNO}_3$  solution, with and without different concentrations from the investigated inhibitors, was determined after 3 hrs of immersion at  $30^{\circ}\text{C}$ . Figure (1) represents this for compound (1) as an example. Similar curves were obtained for other

inhibitors (not shown). Obtained values of % IE are given in Table (2). The presence of inhibitors reduces the corrosion rate of copper specimen in 2 M HNO<sub>3</sub> solution. The % IE was found to increase with increasing the inhibitor concentration. The inhibition achieved by these compounds decreases in the following order: Compound (1) > Compound (2) > Compound (3)

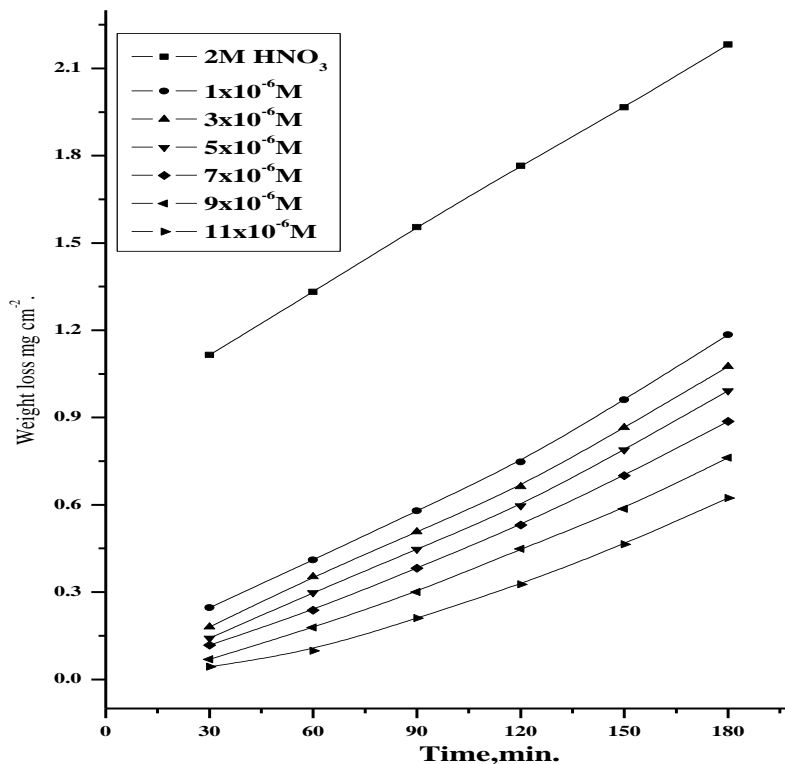


**Figure 1.** weight loss time curves for the dissolution of copper in absence and presence of different concentration of compound (i) at 30°C

**Table 2.** Inhibition efficiency of all compounds at different concentration of compounds as determined from weight loss method at 30°C

Conc., M	Compound ( 1 )			Compound ( 2 )			Compound ( 3 )		
	θ	% IE	C.R.	θ	% IE	C.R.	θ	% IE	C.R.
1 x 10 <sup>-6</sup>	0.588	58.8	3.15	0.557	55.7	3.36	0.520	52.2	1.72
3 x 10 <sup>-6</sup>	0.636	63.6	2.59	0.605	60.5	2.89	0.574	57.4	1.19
5 x 10 <sup>-6</sup>	0.673	67.3	2.22	0.647	64.7	2.48	0.616	61.6	2.78
7 x 10 <sup>-6</sup>	0.711	71.1	1.85	0.701	70.1	2.05	0.664	66.4	2.30
9 x 10 <sup>-6</sup>	0.757	75.7	1.40	0.736	73.6	1.60	0.716	71.6	1.80
11 x 10 <sup>-6</sup>	0.826	82.6	0.92	0.794	79.4	1.02	0.759	75.9	1.37

3.1.2- Adsorption isotherm

One of the most convenient ways of expressing adsorption quantitatively is by deriving the adsorption isotherm that characterizes the metal/inhibitor/ environment system [30]. The values of the degree of surface coverage  $\theta$  were evaluated at different concentrations of the inhibitors in in 2 M HNO<sub>3</sub> solution. Attempts were made to fit  $\theta$  values to various adsorption isotherms. The Temkin adsorption isotherm fits well the experimental data. Plots of  $\theta$  against log C for all concentrations of inhibitors. Figure (2) a straight line relationship in all cases was obtained. This suggests that the adsorption of inhibitors on the copper surface follow Temkin isotherm. It is well known that the standard adsorption free energy ( $\Delta G^{\circ}_{ads}$ ) is related to equilibrium constant of adsorption (K) and  $\Delta G^{\circ}_{ads}$  can be calculated by the following equation [31]:

$$K_{ads} = 1/55.5 \exp [-\Delta G^{\circ}_{ads}/RT] \tag{4}$$

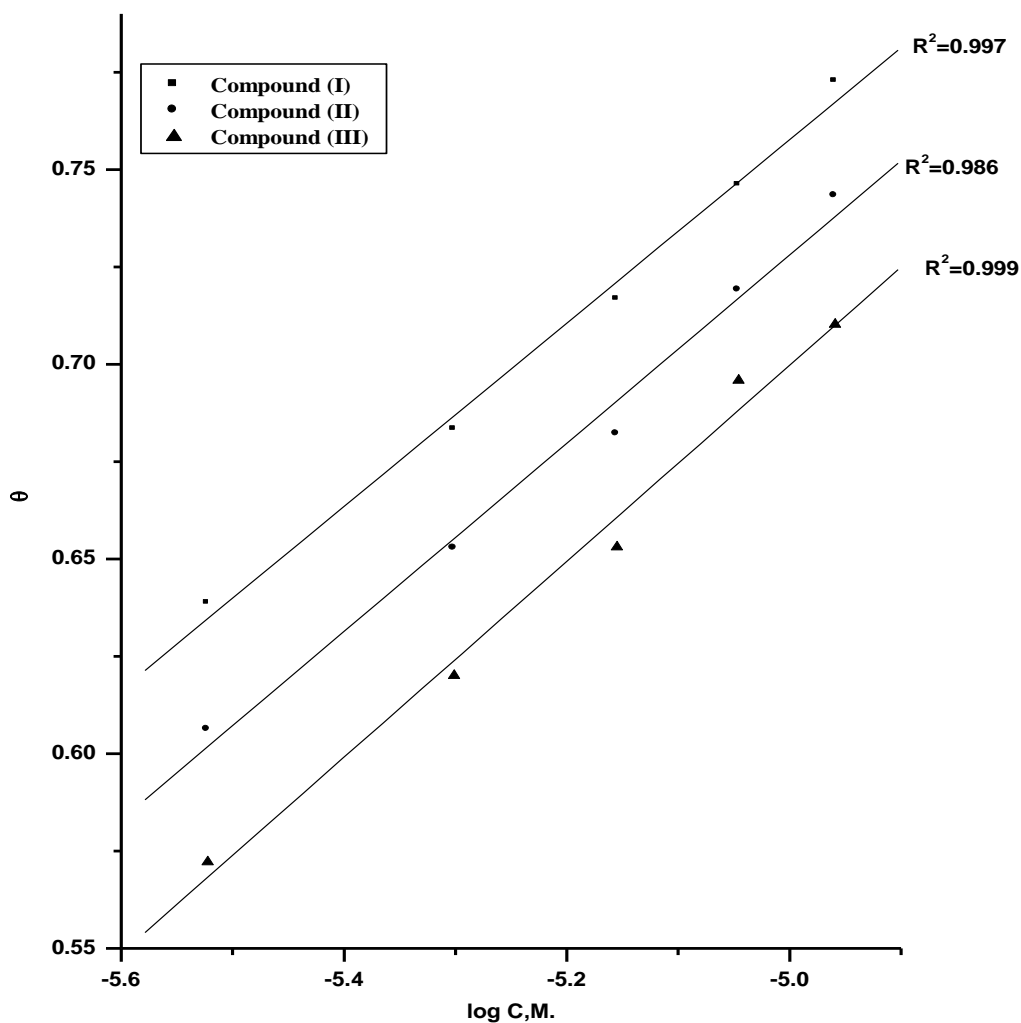


**Figure 2.** Curve fitting of corrosion data for copper in 2M HNO<sub>3</sub> in presence of different concentrations of compounds to the Temkin adsorption isotherm at 30°C

**Table 3.** Inhibitor binding constant ( $K_{ads}$ ), free energy of binding ( $\Delta G^{\circ}_{ads}$ ), number of active sites ( $1/y$ ) and later interaction parameter ( $a$ ) for the compounds for the corrosion of copper in 2 M  $HNO_3$  at 30°C

Inhibitors	Temkin		
	a	$K_{ads} \times 10^8, M^{-1}$	$-\Delta G^{\circ}_{ads}, kJ mol^{-1}$
Compound (1)	12.3	5.98	61.5
Compound (2)	12.2	4.53	60.6
Compound (3)	12.2	3.41	59.7

Figure (2) represents the plot of  $(\theta)$  against  $\log C$  for investigated pharmaceutical compounds. As can be seen from Figure (2), the Temkin isotherm is the best one which explains the experimental results. These results confirm the assumption that, these compounds are adsorbed on the metal surface through the lone pair of electrons of hetero atoms. In addition to, the extent of inhibition is directly related to the performance of adsorption layer which is a sensitive function of the molecular structure. The  $\Delta G^{\circ}_{ads}$  and  $K_{ads}$  values for pharmaceutical compounds were calculated and are recorded in Table (3). The high negative values of  $\Delta G^{\circ}_{ads}$  indicate that these compounds are strongly adsorbed (chemisorption) on copper surface at all the temperature ranges studied but the adsorption decreases with the increase in temperature. The negative values of  $\Delta G^{\circ}_{ads}$  ensure that spontaneity of the adsorption process and the stability of adsorbed layer on the copper surface. The high values of  $K_{ads}$  indicate the strong adsorption of these compounds on copper surface. These values were found to run parallel to the % IE ( $K_1 > K_2 > K_3$ ). This result reflects the increasing capability, due to structural formation, on the metal surface [32].

### 3.1.3- Kinetic parameters

Corrosion reactions are usually regarded as Arrhenius processes and the rate ( $k$ ) can be expressed by equation (5):

$$k = A \exp (E_a^* / RT) \quad (5)$$

where  $E_a$  is the activation energy of the corrosion process  $R$  is the universal gas constant,  $T$  is the absolute temperature and  $A$  is the Arrhenius pre-exponential constant depends on the metal type and electrolyte. Arrhenius plots of  $\log k$  vs.  $1/T$  for copper in 2 M  $HNO_3$  in the absence and presence of different concentrations of inhibitor (1) is shown graphically in Figure (3). Variation of  $\log k$  vs.  $1/T$  is a linear one and the values of  $E_a$  obtained are summarized in Table (4). The effective activation energies show higher values in the presence of inhibitors than in the absence of them. Therefore, the inhibitor retards the corrosion process at lower temperature but this inhibition action is reduced at higher temperature. The calculated effective activation energies show that the investigated compounds inhibits corrosion more effectively at higher concentrations. Also, increase in  $E_a$  with the addition of different concentrations of compounds (1-3) indicating that the energy barrier for the corrosion

reaction increases. It is also indicated that the whole process is controlled by surface reaction, since the activation energy of the corrosion process is over 20 kJ mol<sup>-1</sup> [33].

Enthalpy and entropy of activation ( $\Delta H^*$ ,  $\Delta S^*$ ) are calculated from transition state theory using the equation (6):

$$k = RT/Nh \exp (\Delta S^*/R) \exp (-\Delta H^* / RT) \quad (6)$$

where:  $h$  is Planck's constant,  $N$  is Avogadro's number. A plot of  $\log k/T$  vs  $1/T$  also gave straight lines as shown in Figure (4), for copper dissolution in 2 M HNO<sub>3</sub> in the absence and presence of different concentrations of inhibitor (1). The slopes of these lines equal  $-\Delta H^*/2.303R$  and the intercept equal  $[\log RT/Nh + (\Delta S^*/2.303R)]$  from which the value of  $\Delta H^*$  and  $\Delta S^*$  were calculated and tabulated in Table (4). From these results, it is clear that the presence of the investigated compounds increased the activation energy values and consequently decreased the corrosion rate of the copper. These results indicate that these investigated compounds acted as inhibitors through increasing activation energy of copper dissolution by making a barrier to mass and charge transfer by their adsorption on copper surface. The values of  $\Delta H^*$  reflect the strong adsorption of these compounds on copper surface. The values of  $\Delta S^*$  in the absence and presence of the investigated compounds are large and negative; this indicates that the activated complex in the rate-determining step represents an association rather than dissociation step, meaning that a decrease in disordering takes place on going from reactants to the activated complex and the activated molecules were in higher order state than that at the initial state [34-35].

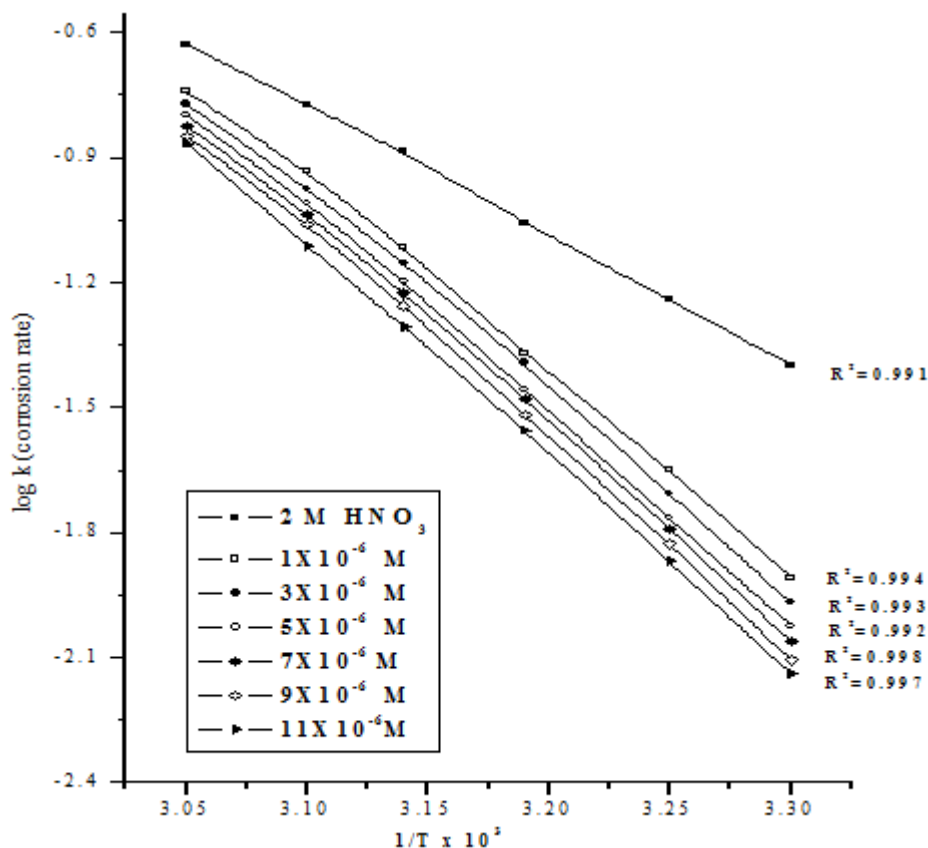


**Figure 3.**  $\log k$  (corrosion rate) –  $1/T$  curves for copper dissolution in 2M HNO<sub>3</sub>, in absence and presence of different concentrations of inhibitor (I)



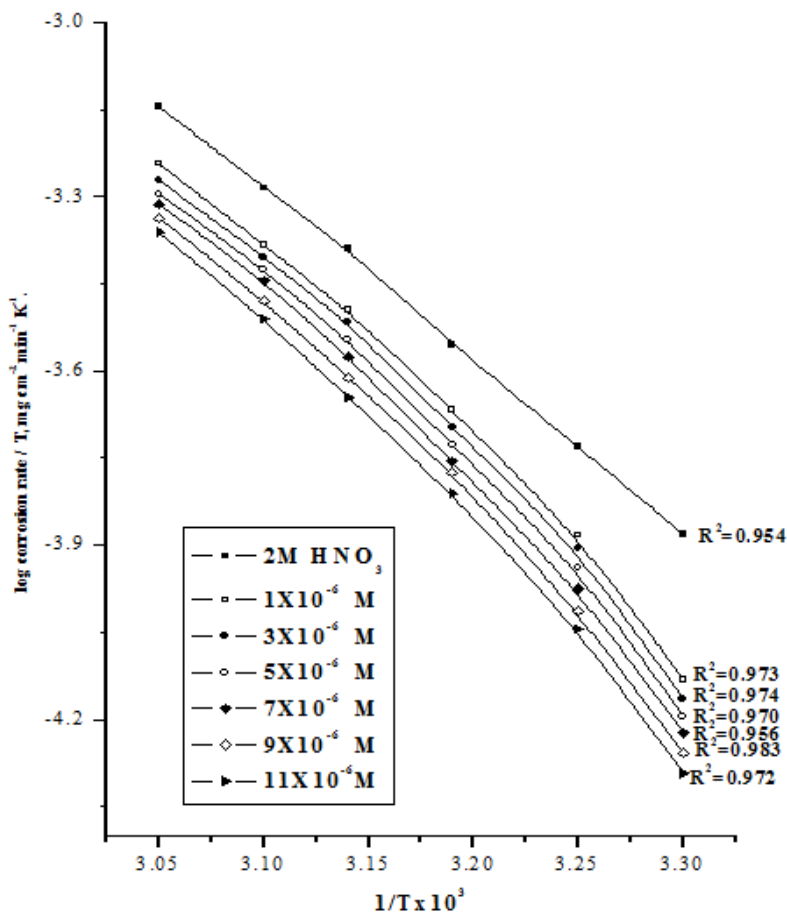


**Figure 4.** log (corrosion rate/T) – (1/T) curves for copper dissolution in 2M HNO<sub>3</sub> absence and presence of different concentrations of inhibitor (I)

**Table 4.** Effect of concentrations of inhibitors on the activation energy, activation enthalpy and activation entropy of copper dissolution in 2 M HNO<sub>3</sub>

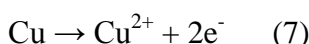
Inhibitor	Concentration, M	E <sub>a</sub> <sup>*</sup> , kJ mol <sup>-1</sup>	ΔH <sup>*</sup> , kJ mol <sup>-1</sup>	-ΔS <sup>*</sup> , J mol <sup>-1</sup> K <sup>-1</sup>
Blank	0.0	51.0	50.7	80.4
1	1×10 <sup>-6</sup>	84.0	85.6	6.3
	3×10 <sup>-6</sup>	92.4	88.2	12.3
	5×10 <sup>-6</sup>	94.0	91.0	19.9
	7×10 <sup>-6</sup>	94.4	90.3	20.5
	9×10 <sup>-6</sup>	95.2	93.2	24.9
	11×10 <sup>-6</sup>	96.0	93.3	24.6
2	1×10 <sup>-6</sup>	78.6	75.8	24.0
	3×10 <sup>-6</sup>	79.0	77.7	18.7
	5×10 <sup>-6</sup>	82.2	79.5	13.3
	7×10 <sup>-6</sup>	83.0	80.3	11.5
	9×10 <sup>-6</sup>	83.0	81.6	7.8
	11×10 <sup>-6</sup>	84.1	82.4	6.4
3	1×10 <sup>-6</sup>	66.8	70.4	40.0
	3×10 <sup>-6</sup>	73.1	70.9	35.7
	5×10 <sup>-6</sup>	74.2	73.0	32.4
	7×10 <sup>-6</sup>	75.8	74.4	27.5
	9×10 <sup>-6</sup>	77.2	78.3	16.3
	11×10 <sup>-6</sup>	79.2	79.2	12.3

### 3.2. Potentiodynamic polarization measurements

According to corrosion theory [36], the rightward shift of the cathodic curves reveals that corrosion is mainly accelerated by cathode reactions. Hence, HNO<sub>3</sub> is a strong copper oxidizer capable of rapidly attacking copper. In addition to, the Tafel polarization curves exhibit no steep slope in the anodic range, meaning that no passive films are formed on the copper surface. Consequently, copper may directly dissolve in 2 M HNO<sub>3</sub> solutions. As known, from Pourbaix diagram for copper-water system [37-38] that the copper is corroded to Cu<sup>2+</sup> in nitric acid solutions, and no oxide film is formed to protect the surface from corrosion. The electrochemical reactions for copper in nitric acid solution can be described as follows:

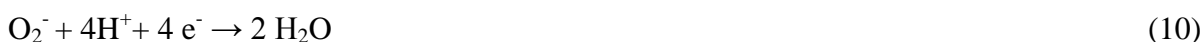
Anodic reaction:

The dissolution of copper is controlled by diffusion of soluble Cu (II) species from the outer Helmholtz plane to the bulk solution.



Cathodic reactions:

The corrosion of copper in nitric acid involves reduction of the nitrate ion (Eqs.(8) and (9)). In aerated nitric acid solutions, dissolved oxygen may also be reduced on copper surface [39] (Eq. (13)).



The cathodic and anodic polarization curve for copper corrosion in the absence and in the presence of various concentrations of the investigated inhibitors at 30 ± 1°C was studied. It shows that with increasing concentrations of each compound, the corrosion current density  $j_{\text{corr}}$  decreased considerably as compared to the blank and the efficiency is increased as the inhibitor concentration is increased. It is observed that, in all cases, increase in inhibitor concentration reduces both the anodic and cathodic current densities. Fig. (5) which show Tafel polarization behavior of copper in nitric acid without and with the addition of different concentrations of the Pharmaceutical Compounds.

The electrochemical kinetic parameters of corrosion such as corrosion current density  $j_{\text{corr}}$ , corrosion potential  $E_{\text{corr}}$ , corrosion rate CR, anodic Tafel constants  $\beta_a$ , cathodic Tafel constants  $\beta_c$  and inhibition efficiency %  $\text{IE}_{\text{Tafel}}$  were calculated from dc curves and presented in Table (5). It is observed from Table 2 that the addition of any of the studied pharmaceutical compounds in the concentration range  $1 \times 10^{-6}$  to  $11 \times 10^{-6}$  M reduces the dissolution rate of copper. It can also be seen from Table (5), that anodic and cathodic Tafel slopes were approximately constant, meaning that the inhibiting action of these compounds occurred by simple blocking of the available surface area. In other words, the inhibitors decreased the surface area available for anodic dissolution and oxygen reduction without affecting the reaction mechanism.

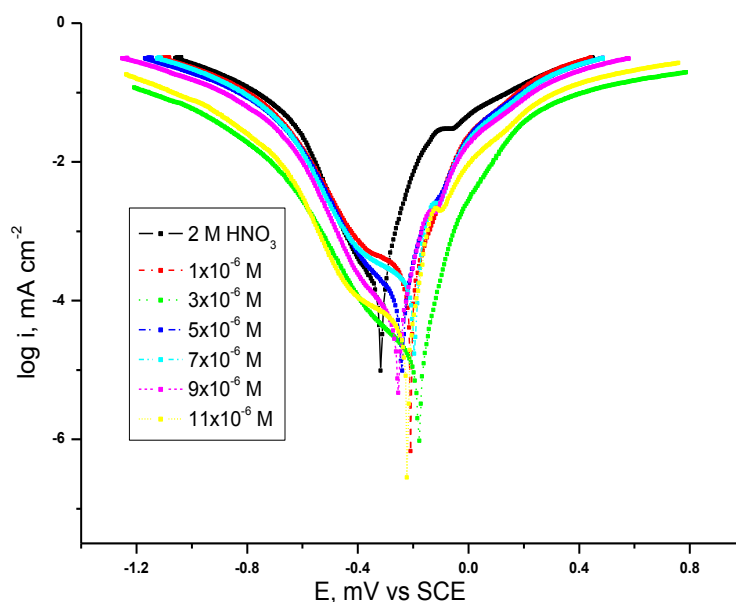


**Figure 5.** Potentiodynamic polarization curves for the dissolution of copper in 2 M HNO<sub>3</sub> in the absence and presence of different concentrations of compound (1) at 30 °C

**Table 5.** The effect of concentration of the investigated compounds on the free corrosion potential ( $E_{corr}$ ), corrosion current density ( $i_{corr}$ ), Tafel slopes ( $\beta_a$  &  $\beta_c$ ), inhibition efficiency (% IE), degree of surface coverage ( $\theta$ ) and corrosion rate for the corrosion of copper in 2 M HNO<sub>3</sub> at 30 °C

Comp.	Conc., M M	$-E_{corr.}$ , mV vs SCE	$i_{corr.}$ , $\mu A\ cm^{-2}$	$\beta_a$ , mV dec <sup>-1</sup>	$\beta_c$ , mV dec <sup>-1</sup>	$\theta$	% IE	C.R. mmy <sup>-1</sup>
1	Blank	226	1290	392	163	----	-----	5.5
	$1 \times 10^{-6}$	254	777	277	140	0.398	39.8	3.2
	$3 \times 10^{-6}$	253	650	220	196	0.496	49.6	2.7
	$5 \times 10^{-6}$	262	640	174	185	0.504	50.4	2.6
	$7 \times 10^{-6}$	267	522	163	237	0.596	59.6	2.2
	$9 \times 10^{-6}$	269	369	187	256	0.714	71.4	1.5
	$11 \times 10^{-6}$	246	133	234	256	0.897	89.7	0.6
2	$1 \times 10^{-6}$	254	899	151	273	0.381	38.1	3.3
	$3 \times 10^{-6}$	256	682	284	206	0.471	47.1	2.7
	$5 \times 10^{-6}$	265	677	245	146	0.475	47.5	2.6
	$7 \times 10^{-6}$	253	522	204	178	0.595	59.5	2.1

	$9 \times 10^{-6}$	262	492	247	158	0.619	61.9	2.0
	$11 \times 10^{-6}$	277	186	179	217	0.856	85.6	0.7
3	$1 \times 10^{-6}$	244	868	395	134	0.327	32.7	3.9
	$3 \times 10^{-6}$	253	765	273	148	0.407	40.7	3.2
	$5 \times 10^{-6}$	256	688	322	135	0.466	46.6	2.7
	$7 \times 10^{-6}$	258	601	272	116	0.534	53.4	2.6
	$9 \times 10^{-6}$	261	503	297	104	0.610	61.0	2.1
	$11 \times 10^{-6}$	278	454	191	128	0.648	64.8	1.8

No definite shift in corrosion potential,  $E_{\text{corr}}$ , was observed in the presence of the inhibitor as compared to uninhibited solution thereby suggesting that Pharmaceutical Compounds may be classified as mixed-type inhibitors. The %IE was also found to increase with increasing the inhibitor concentration. The inhibition achieved by these compounds decreases in the following order: Compound (1) > Compound (2) > Compound (3)

### 3.3. Electrochemical impedance spectroscopy measurements

Nyquist impedance plots obtained for the copper electrode at respective corrosion potentials after 30 min immersion in 2 M  $\text{HNO}_3$  in presence and absence of various concentrations compound (1) as shown in Figure (6). Similar curves were obtained for other compounds (not shown). This diagram exhibits a single semi-circle shifted along the real impedance ( $Z_r$ ) axis. This diagrams show single capacitive loop, which is attributed to charge transfer of the corrosion process, and the diameters of the loops increase with the increase of concentrations. It was observed from the obtained EIS data that  $R_{\text{ct}}$  increases and  $C_{\text{dl}}$  decreases with the increasing of inhibitor concentrations. The increase in  $R_{\text{ct}}$  values, and consequently of inhibition efficiency, may be due to the gradual replacement of water molecules by the adsorption of the inhibitor molecules on the metal surface to form an adherent film on the metal surface, and this suggests that the coverage of the metal surface by the film decreases the double layer thickness. Also, this decrease of  $C_{\text{dl}}$  at the metal/solution interface with increasing the inhibitor concentration can result from a decrease in local dielectric constant which indicates that the inhibitors were adsorbed on the surface at both anodic and cathodic sites [43]. The analysis of Nyquist plots from experimental data is done by using the circuit in Fig. (7), in which  $R_s$  represents the electrolyte resistance,  $R_{\text{ct}}$  represents the charge-transfer resistance and the constant phase element (CPE). .

The impedance data confirm the inhibition behavior of the inhibitors obtained with other techniques.

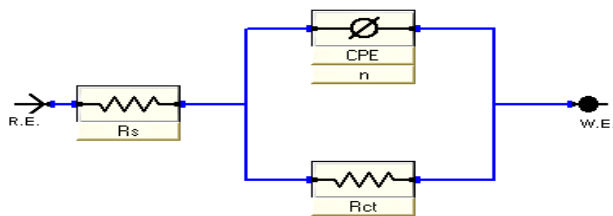


Figure 7. Equivalent circuit used to model impedance data in 2 M HNO<sub>3</sub> solutions

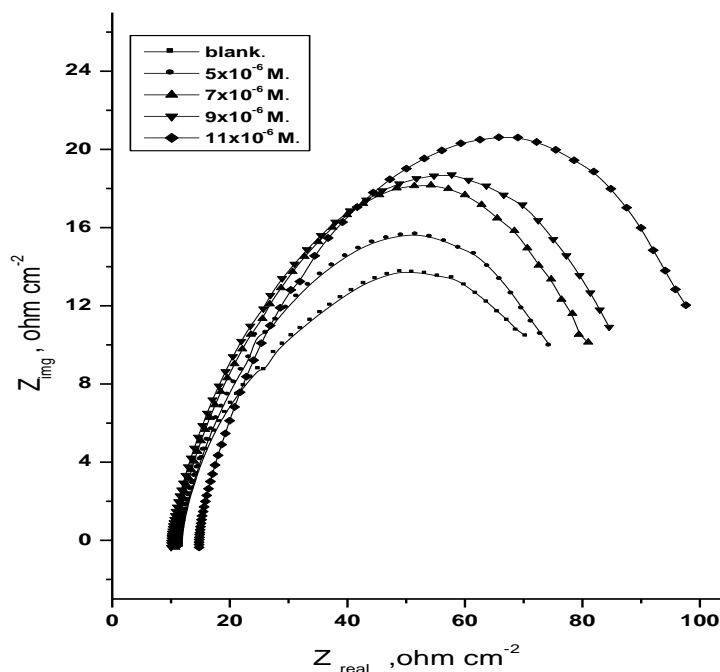


Figure 6. The Nyquist plot for corrosion of copper in 2 M HNO<sub>3</sub> in the absence and presence of different concentrations of compound (1) at 30°C

Table 6. Electrochemical kinetic parameters obtained from EIS technique for copper in 2 M HNO<sub>3</sub> without and with various concentrations of investigated compounds

Compound	Conc., (M)	R <sub>s</sub> , Ω cm <sup>2</sup>	Y <sub>0</sub> , × 10 <sup>-3</sup> μΩ <sup>-1</sup> s <sup>n</sup> cm <sup>-2</sup>	n	R <sub>ct</sub> , Ω cm <sup>2</sup>	C <sub>dl</sub> , μFcm <sup>-2</sup>	θ	% IE
<b>Blank</b>	0.0	10.9	3.27	0.46	71.4	608.7	-	-
<b>1</b>	5x10 <sup>-6</sup>	11.2	2.20	0.57	85.5	623.9	0.165	16.5
	7x10 <sup>-6</sup>	11.1	1.98	0.55	112.6	603.4	0.366	36.6
	9x10 <sup>-6</sup>	11.1	1.87	0.51	147.7	548.6	0.517	51.7
	11x10 <sup>-6</sup>	12.2	1.69	0.50	180.8	519.1	0.605	60.5
<b>2</b>	5x10 <sup>-6</sup>	10.8	2.67	0.50	93.5	702.9	0.237	23.7
	7x10 <sup>-6</sup>	11.0	2.41	0.49	108.5	609.6	0.342	34.2
	9x10 <sup>-6</sup>	12.1	2.39	0.50	119.0	709.3	0.400	40.0
	11x10 <sup>-6</sup>	11.0	2.22	0.49	126.3	607.0	0.435	43.5
<b>3</b>	5x10 <sup>-6</sup>	11.0	2.67	0.51	77.2	588.3	0.076	7.6
	7x10 <sup>-6</sup>	10.2	2.13	0.53	81.1	454.5	0.120	12.0
	9x10 <sup>-6</sup>	9.4	2.11	0.52	95.9	501.5	0.256	25.6
	11x10 <sup>-6</sup>	14.0	1.81	0.52	105.2	407.3	0.322	32.2

3.4. Electrochemical Frequency Modulation measurements

In corrosion research, it is known that the corrosion process is non-linear in nature, a potential distortion by one or more sine waves will generate responses at more frequencies than the frequencies of applied signal. Virtually no attention has been given to the intermodulation or electrochemical frequency modulation. However, EFM showed that this non-linear response contains enough information about the corroding system so that the corrosion current can be calculated directly. The great strength of the EFM is the causality factors which serve as an internal check on the validity of the EFM measurement. With the causality factors the experimental EFM data can be verified.

Figures (8-12) show the current response contains not only the input frequencies, but also contains frequency components which are the sum, difference, and multiples of the two input frequencies. The larger peaks were used to calculate the corrosion current density ( $i_{corr}$ ), the Tafel slopes ( $\beta_a$  and  $\beta_c$ ) and the causality factors (CF-2 and CF-3). These electrochemical corrosion kinetic parameters at different concentrations of pharmaceutical compounds in 2 M HNO<sub>3</sub> at 30°C were listed in Table (7). The inhibition efficiency % IE, calculated from equation (12), increase by increasing the studied inhibitor concentrations.

$$\% IE_{EFM} = [1 - (i_{corr} / i^{\circ}_{corr})] \times 100 \tag{12}$$

where  $i^{\circ}_{corr}$  and  $i_{corr}$  are corrosion current densities in the absence and presence of inhibitors, respectively. The causality factors CF-2 and CF-3 in Table (6) are close to their theoretical values of 2.0 and 3.0, respectively indicating that the measured data are of good quality. The calculated inhibition efficiency obtained from weight loss, Tafel polarization and EIS measurements are in good agreement with that obtained from EFM measurements.

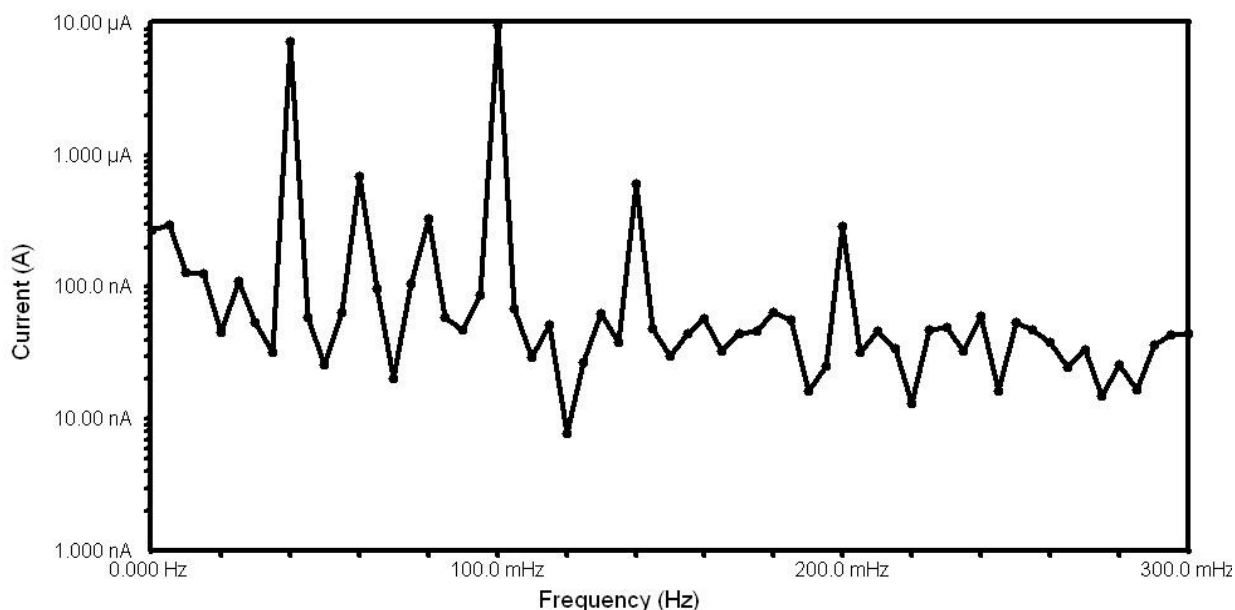
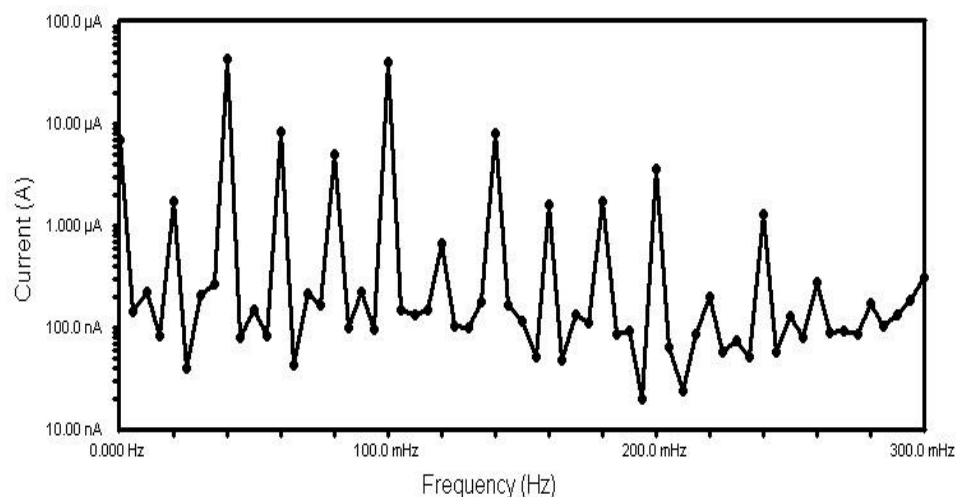
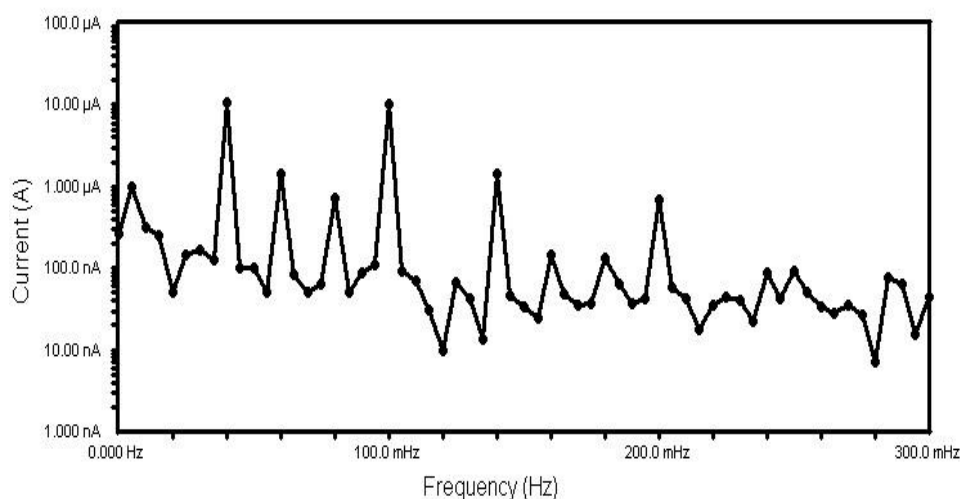


Figure 8. Intermodulation spectra for copper in 2 M HNO<sub>3</sub> alone



**Figure 9.** Intermodulation spectra for copper in 2 M HNO<sub>3</sub> + 5x10<sup>-6</sup> M of compound (1) .



**Figure 10.** Intermodulation spectra for copper in 2 M HNO<sub>3</sub>+ 7x10<sup>-6</sup> M of compound (1)

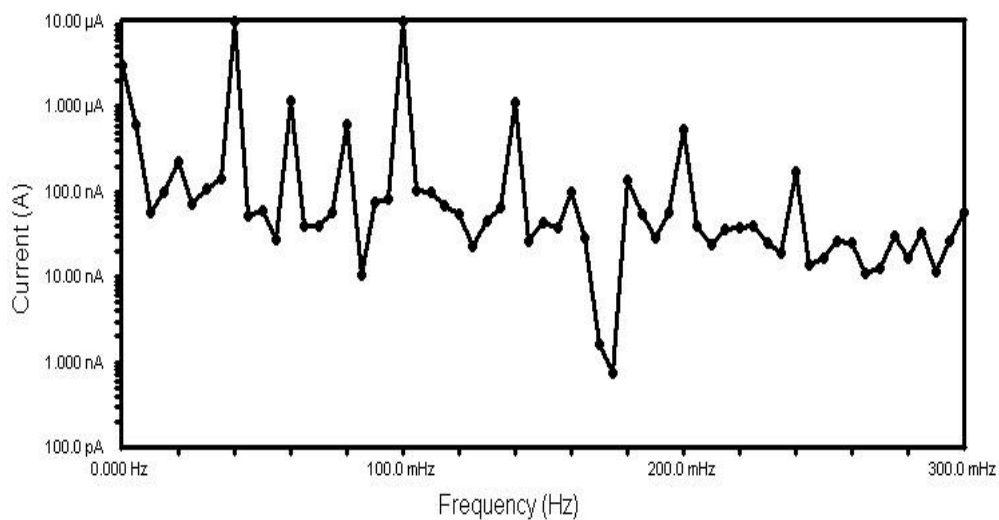


**Figure 11.** Intermodulation spectra for copper in 2 M HNO<sub>3</sub> + 9x10<sup>-6</sup> M of compound (1)

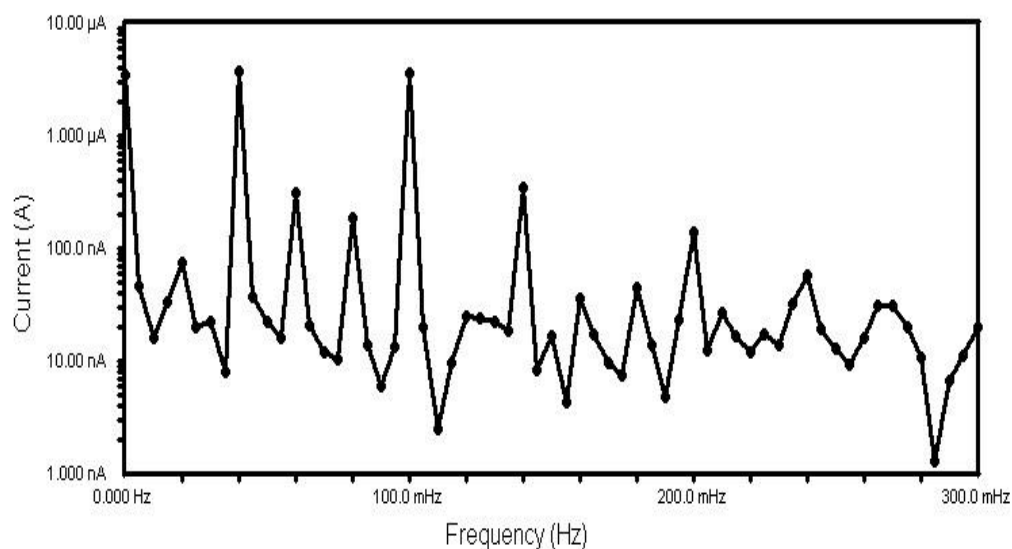


**Figure 12.** Intermodulation spectra for copper in 2 M HNO<sub>3</sub> + 11x10<sup>-6</sup> M of compound (1)

**Table 7.** Electrochemical kinetic parameters obtained by EFM technique for copper in 2 M HNO<sub>3</sub> in the absence and presence of different concentrations of pharmaceutical compounds

Inhibitor	Conc., M	$i_{corr.}$ , $\mu\text{A cm}^2$	$\beta_a$ , mV dec <sup>-1</sup>	$\beta_c$ , mV dec <sup>-1</sup>	CF-2	CF-3	% IE
Blank	0.0	22.12	164	244	2.07	3.01	-----
1	5X10 <sup>-6</sup>	10.19	33	76	1.91	3.04	<b>53.9</b>
	7X10 <sup>-6</sup>	8.24	48	99	1.98	3.08	<b>62.8</b>
	9x10 <sup>-6</sup>	6.62	88	108	2.00	3.03	<b>70.1</b>
	11x10 <sup>-6</sup>	4.297	61	65	1.97	2.89	<b>80.6</b>
2	5X10 <sup>-6</sup>	13.39	34	92	1.89	2.91	<b>39.5</b>
	7X10 <sup>-6</sup>	11.39	47	115	2.02	3.05	<b>48.5</b>
	9x10 <sup>-6</sup>	9.07	110	122	1.78	2.98	<b>59.0</b>
	11x10 <sup>-6</sup>	7.27	80	98	2.02	3.01	<b>67.1</b>
3	5X10 <sup>-6</sup>	14.44	43	120	1.93	3.03	<b>34.7</b>
	7X10 <sup>-6</sup>	11.85	39	71	1.88	3.08	<b>46.4</b>
	9x10 <sup>-6</sup>	10.30	42	100	2.01	3.02	<b>53.4</b>
	11x10 <sup>-6</sup>	7.99	48	71	1.91	2.89	<b>63.9</b>



### 3.5. Quantum Chemical study

Quantum chemical calculations have proved to be a very powerful tool for studying corrosion inhibition mechanism [44, 45]. There is a number of satisfactory correlations have been reported by other investigators [46-47] between the inhibition efficiency of inhibitors used and some quantum chemical parameters that can be related to the metal-inhibitor interaction namely: highest occupied molecular orbitals,  $E_{\text{HOMO}}$ , lowest unoccupied molecular orbital,  $E_{\text{LUMO}}$ , energy gap,  $\Delta E = E_{\text{LUMO}} - E_{\text{HOMO}}$ .

The energy gap ( $\Delta E$ ) is an important parameter as a function of reactivity of the inhibitor molecule towards the adsorption on metallic surface. Low values of the energy gap will yield good inhibition efficiencies, because the energy needed to remove an electron from the last occupied orbital will be low [48]. According to Frontier molecular orbital theory of chemical reactivity, transition of electron is due to an interaction between frontiers orbitals-highest occupied molecular orbital HOMO and lowest unoccupied molecular orbital LUMO of reacting species [49-51]. The higher the HOMO energy of the inhibitor, the greater the trend of offering electrons to unoccupied d-orbital of the metal, and the higher the corrosion inhibition efficiency. The lower the LUMO energy, the easier the acceptance of electrons from metal surface [52]

Table (8) shows some of quantum chemical parameters were computed using the PM3 semiempirical method. These quantum chemical properties were obtained after complete geometrical optimizations of the investigated molecules with respect to the all nuclear coordinates using density functional theory (DFT).

It can be seen that all calculated quantum chemical parameters of the three compounds studied validate these experimental results.

**Table 8.** The calculated quantum chemical parameters of the investigated pharmaceutical compounds

Parameters	1	2	3
$-E_{\text{HOMO}}$ (eV)	9.114	9.342	9.386
$-E_{\text{LUMO}}$ (eV)	1.056	0.126	0.110
<b>Molecular weight</b>	297.7	217.3	198.2
$\Delta E$ (eV)	8.058	9.216	9.276

## 4. INHIBITION MECHANISM

Inhibition of the copper corrosion in 2 M  $\text{HNO}_3$  by the investigated pharmaceutical compounds as indicated by weight loss, potentiodynamic polarization and other methods were found

to depend on the number of adsorption sites in the molecule and their charge density, molecular size and stability of these additives in acidic solution. The observed corrosion data in presence of these inhibitors, namely: i) The decrease of corrosion rate and corrosion current with increase in concentration of the inhibitor ii) The linear variation of weight loss with time iii) The shift in Tafel lines to higher potential regions iii) The decrease in corrosion inhibition with increasing temperature indicates that desorption of the adsorbed inhibitor molecules takes place iv) The inhibition efficiency was shown to depend on the number of adsorption active centers in the molecule and their charge density. The corrosion inhibition is due to adsorption of the inhibitors at the electrode/ solution interface, the extent of adsorption of an inhibitor depends on the nature of the metal, the mode of adsorption of the inhibitor and the surface conditions. Adsorption on copper surface is assumed to take place mainly through the active centers attached to the inhibitor and would depend on their charge density. It was concluded that the mode of adsorption depends on the affinity of the metal towards the  $\pi$ -electron clouds of the ring system. Metals such as copper, which have a greater affinity towards aromatic moieties, were found to adsorb benzene rings in a flat orientation. The order of decreasing the percentage inhibition efficiency of the investigated inhibitors in the corrosive solution was as follow: compound (1) > compound (2) > compound (3)

Compound (1) exhibits excellent inhibition power due to: (i) its larger molecular size (297.74) that may facilitate better surface coverage, (ii) its adsorption through 9 centers of adsorption (4-O, 2-S, 3-N atoms) and iii) The lone pair of Cl atom are shared with phenyl group, it becomes a donor by mesomeric effect and increase the electron density on compound (1). Compound (2) comes after compound (1) in inhibition efficiency, because it has lesser molecular size (217.29) and lesser number of active centers (5 centers, 3-O, 1-S and 1-N atoms). Compound (3) has the lowest inhibition efficiency. This is due to it's the lowest molecular size (198.22) and lowest number of adsorption centers (4 centers only, 4-O atoms).

## 5. CONCLUSIONS

Based on the above results of this study, the following conclusions can be drawn:

1. The studied Pharmaceutical Compounds are effective inhibitors of corrosion of copper exposed to 2 M HNO<sub>3</sub> solution.
2. Each one of these compounds inhibited corrosion by adsorption mechanism, and the adsorption of the Pharmaceutical Compounds on copper obeys the Temkin adsorption isotherm model.
3. The potentiodynamic polarization studied reveal that Pharmaceutical Compounds examined acted as mixed type inhibitor in 2 M HNO<sub>3</sub>.
4. The results obtained from the four methods are in reasonably good agreement.
5. The theoretical PM3 calculations support the experimental results.
6. The applied techniques showed that compound (1) among the tested pharmaceutical compounds, produced the best protection against copper corrosion in nitric acid solution.

## References

1. K.F. Khaled, Sahar A. Fadel-Allah, B. Hammouti, *Mat. Chem. Phys.* 117(2009) 148.
2. M.M. El-Naggar, *Corros. Sci.* 42(2000) 773.
3. Woo-Jin Lee, *Mat. Sci. and Eng.* A348 (2003), 217.
4. S.A. Abd El-Maksoud, A.A. El-Shafei, H.A. Mostafa, A.S. Fouda, *Mater. And Corros.* 46(1995)468.
5. S. Abd El-Waness, *Anti-Corros. Methods Mater.*, 41(1994), 3.
6. L.M. Madkour, M.A. Elmorsi, M. M. Ghoneim, *Monat. Chem.* 126(1995), 1087.
7. S.A. Abd El-Maksoud, H.H. Hassan, *Mater. Corros.* 58(2007), 369.
8. A.S. Fouda, A. Abd El-Aal, A.B. Kandil, *Desalination.* 201(2006), 216.
9. A.K. Maayta, M.B. Bitar, M.M. Al-Abdallah, *Br. Corros. J.* 36(2001), 133.
10. M. Khodari, M.M. Abou-krisa, F.H. Assaf, F.M. El-Cheikh, A.A. Hussien, *Mat. Chem. Phys.* 71(2001), 279.
11. G. Trabaneli, *Corrosion.* 47(1991), 410.
12. F. Zucchi, G. Trabaneli, C. Monticelli, *Corros. Sci.* 38(1996), 147.
13. M. Ohsawa, W. Suetaka, *Corros. Sci.* 19(1979), 709.
14. V. Lakshminarayanan, R. Kannan, S.R. Rajagopalan, *J. Electroanal. Chem.*, 364(1994), 79.
15. F. Ammeloot, C. Fiaud, E.M.M. Sutter, *Electrochem. Acta.* 42(1997), 4565.
16. I. Ignat, S. Varvara, L. Muresan, *Studia Univ. Babeş-Bolyai, Chemia L1* (2006) 127.
17. L. Ying, F. Hailtao, Z. Yifan, W. Wuji. *J. Mater. Sci.* 38(2003), 407.
18. Orlin Blajiev, Annick Hubin, *Electrochimica Acta.* 49(2004), 2761.
19. E.M. Sherif, Su-Moon Park, *Electrochimica Acta.* 51(2006), 6556.
20. El-Sayed M. Sherif, *Applied surface science.* 252(2006), 8615.
21. E.M. Sherif, Su-Moon Park, *Corrosion science.* 48(2006), 4065.
22. El-Sayed M. Sherif, A.M.Shamy, Mostafa M.Ramla, Ahmed O.H.El Nazhawy, *Materials chemistry and physics.*102(2007), 231.
23. L. Valek, S. Martinez, *Mater. Lett.* 61(2007), 148.
24. S. El Issami, L. Bazzi, M. Mihit, M. Hilali, R. Salghi, E. Ait Addi, *Ann. Chim. Sci. Mater.* 27(2002), 63.
25. R. Salghi, L. Bazzi, B. Hammouti, A. Bouchart, S. Kertit, E. Ait Addi, Z. El Alami, *Ann. Chim. Sci. Mater.* 27(2002),187.
26. A. Dafali, B. Hammouti, A. Aouniti, R. Mokhlisse, S. Kertit, K. El Kacemi, *Ann. Chim. Sci. Mater.* 22(2000), 437.
27. A. Dafali, B. Hammouti, S. Kertit, *J. Electrochem. Soc. Ind.* 50(2001), 62.
28. R. Ravichandran, N. Rajendran, *Appl. Surf. Sci.* 241(2005), 449.
29. R.W. Bosch, J. Hubrecht, W.F. Bogaerts, B.C. Syrett, *Corrosion.* 57(2001), 60.
30. E.Khamis, *Corrosion*, 46 (1990) 476.
31. I.K. Putilova, S.A. Balizen, Y.P. Barasanik, *Metallic corrosion inhibitors, Pergamon Press. Oxford.* (1960) 30.
32. F. L. Laque and H. R. Gapson; *Corrosion resistance of metals and alloys*; 2nd ed., Reinhold publishing corporation, New York, (1963).
33. S. N. Banerjee, " An introduction to science of corrosion and its inhibition" Ox-anion Press, Pvt Ltd., New Delhi, (1985).
34. L. Riggs and R. M. Hurd; *Corrosion*; 23 (1967) 252.
35. M. K. Gomma and M. H. Wahdan; *Mater. Chem. Phys.* 39 (1995) 209.
36. D.A. Jones, *Principles and Prevention of Corrosion*, second ed., Prentice Hall, Upper Saddle River, NJ, (1983).
37. M. Pourbaix, *Atlas of Electrochemical Equilibria in Aqueous Solutions*, NACE, Houston, TX, (1975).

38. H.E. Johnson, *J. Electrochem. Soc.* 112(1965), 638.
39. W.H. Smyrl, in: J.O.M. Bockris, B.E. Conway, E. Yeager, R.E. White (Eds.), *Comprehensive Treatise of Electrochemistry*, vol. 4, Plenum Press, New York. (1981), 116.
40. M. Kendig, S. Jeanjaquet, *J. Electrochem. Soc.* 149( 2002), 47.
41. F. Mansfeld, M.W. Kendig, S. Tsai, *Corros.* 38 (1982) 570.
42. F. Mansfeld, *Electrochim. Acta*, 35 (1990) 1533.
43. E. McCafferty, N Hackerman, *J. Electrochem. Soc.* 119 (1972) 146.
44. D.X. Wang, S.Y. Li, Y. Ying, M.J. Wang, H.M. Xiao, Zh.X. Chen, *Corros. Sci.*, 41 (1999) 1911.
45. G. Bereket, C. Ög̃retir, C. Özs, ahin, *J. Mol. Struct. (THEOCHEM)* 663 (2003) 39.
46. Lukovits I, Kalman E, Palinkas G *Corrosion* .51(1995), 201.
47. Sastri Vs, perumareddi JR *Corrosion* .53(1997), 617.
48. KF. Khaled *Electrochim Acta* .48(2003), 2635.
49. H. Fujikamoto, S. Yamabe, K. Fukui, *J. Chem. Phys.* 60(1974) 572.
50. J. Fang, J. Li, *J. Mol. Struct. (THEOCHEM)* .593 (2002) 179.
51. G. Bereket, E. Hu̇ r, C. Ȯ g̃retir, *J. Mol. Struct. (THEOCHEM)*,.578 (2002)79.
52. I. Lukovits, K. Palfi, E. Kalman, *Corrosion* .53 (1997) 915.